ORIGINAL PAPER

Seismicity and source parameters of moderate earthquakes in Sikkim Himalaya

Pinki Hazarika · M. Ravi Kumar

Abstract In this study, we accurately relocate 360 earthquakes in the Sikkim Himalaya through the application of the double-difference algorithm to 4 years of data accrued from a eleven-station broadband seismic network. The analysis brings out two major clusters of seismicity—one located in between the main central thrust (MCT) and the main boundary thrust (MBT) and the other in the northwest region of Sikkim that is site to the devastating Mw6.9 earthquake of September 18, 2011. Keeping in view the limitations imposed by the Nyquist frequency of our data (10 Hz), we select 9 moderate size earthquakes ($5.3 \geq Ml \geq 4$) for the estimation of source parameters. Analysis of shear wave spectra of these earthquakes yields seismic moments in the range of 7.95×10^{21} dyne-cm to 6.31×10^{23} dyne-cm and corner frequencies in the range of 1.8–6.25 Hz. Smaller seismic moments obtained in Sikkim when compared with the rest of the Himalaya vindicates the lower seismicity levels in the region. Interestingly, it is observed that most of the events having larger seismic moment occur between MBT and MCT lending credence to our observation that this is the most active portion of Sikkim Himalaya. The estimates of stress drop and source radius range from 48 to 389 bar and 0.225 to 0.781 km, respectively. Stress drops do not seem to correlate with the scalar seismic moments affirming the view that stress drop is independent over a wide moment range. While the continental collision scenario can be invoked as a reason to explain a predominance of low stress drops in the Himalayan region, those with relatively higher stress drops in Sikkim Himalaya could be attributed to their affinity with strike-slip source mechanisms. Least square regression of the scalar seismic moment (M_0) and local magnitude (Ml) results in a relation $\text{Log} M_0 = (1.56 \pm 0.05)Ml + (8.55 \pm 0.12)$ while that between moment magnitude (M_w) and local magnitude as $M_w = (0.92 \pm 0.04)Ml + (0.14 \pm 0.06)$. These relations could serve as useful inputs for the assessment of earthquake hazard in this seismically active region of Himalaya.

Keywords Seismicity · Source parameters · Sikkim Himalaya · hypoDD

P. Hazarika (✉) · M. Ravi Kumar
National Geophysical Research Institute (CSIR), Hyderabad, India
e-mail: pinki@ngri.res.in

1 Introduction

The Himalayan orogenic belt is acknowledged as one of the most seismically active continental collision zones in the world, being host to several destructive large earthquakes since historic times. Interestingly, the Sikkim region that constitutes a part of the eastern Himalayan arc has only experienced moderate size earthquakes. Prior to 2011, the largest earthquake that occurred in the region was in the year 1988 with a magnitude of M6.6 and a reported intensity of VII. Recently, on September 18, 2011, a devastating earthquake of Mw 6.9 that claimed at least 100 lives occurred to the northwest of Sikkim, close to the border between India and Nepal. This earthquake with a focal depth of about 50 km has its epicenter at 27.72°N and 88.14°E (USGS). A description of this earthquake, including the damage to the landscape and engineering structures, the seismotectonic scenario and the discrepancies in the hypocentral locations reported by various agencies, has been succinctly documented by Rajendran et al. (2011) and Kayal et al. (2011). The strike-slip nature of the 2011 Sikkim earthquake reiterates the dominance of transverse tectonics in the regions of Sikkim and Bhutan (Hazarika et al. 2010; Drukpa et al. 2006), in contrast to a thrust environment prevalent in other segments of the Himalaya owing to shallow underthrusting of the Indian tectonic plate beneath Eurasia along the plane of detachment.

The major thrust zones in the Sikkim region are the Main Boundary Thrust (MBT), Main Central Thrust (MCT) and Main Frontal Thrust (MFT). While the MBT and MCT are near parallel in the rest of the Himalaya, the MCT takes a peculiar overturn in the Sikkim Himalaya. Apart from these major thrust belts, the other tectonic features in this region are the sub-parallel NW–SE trending Tista and Gangtok lineaments and the SW–NE-oriented Kanchanjangha fault in the north (Fig. 1). Interestingly, the Sikkim region has a distinct tectonic scenario when compared with the rest of the Himalaya. While the entire Himalayan front is predominantly characterized by shallow-angle thrust faulting, this region seems to be governed by transverse tectonics evidenced by focal mechanisms that indicate a dextral motion along the northwest-trending Tista and Gangtok lineaments. Most of the Sikkim region has a relatively flat topography, unlike in the rest of the Himalayan mountain chain, probably due to lower rates of convergence in the recent geologic past. It is proposed that crustal shortening in the Sikkim Himalaya has been substantially accommodated by transverse tectonics rather than underthrusting in recent times (Hazarika et al. 2010). Although recent studies using local networks have enabled placing tight constraints on the spatial trends in seismicity (Hazarika et al. 2010), studies related to the source parameters in Sikkim Himalaya are still sparse. The present study is aimed at updating the seismicity patterns in the region through a comprehensive analysis of 5 years of local earthquake waveforms, estimating the source parameters of the moderate-sized earthquakes, such as seismic moment, corner frequency, stress drop, source radius and understand their bearing on the seismotectonics of the Sikkim Himalaya.

Determination of earthquake source parameters like stress drop, corner frequency, source radius and scalar seismic moment is important to assess the seismic hazard potential of a tectonically active region like the Himalaya, since they quantify the nature and strength of energy release during the rupture process. Spectral analysis of local and regional earthquake waveforms to characterize the frequency dependence of ground motion amplitudes has been a standard practice to measure the earthquake size (resulting from fault slip) and rupture dimensions in terms of scalar seismic moment and corner frequency, respectively, assuming an omega-square model for the source dislocation (Aki 1967; Brune 1970, 1971; Boatwright 1980). Another important source parameter is the stress drop, which signifies the difference between the ambient stress across a fault before
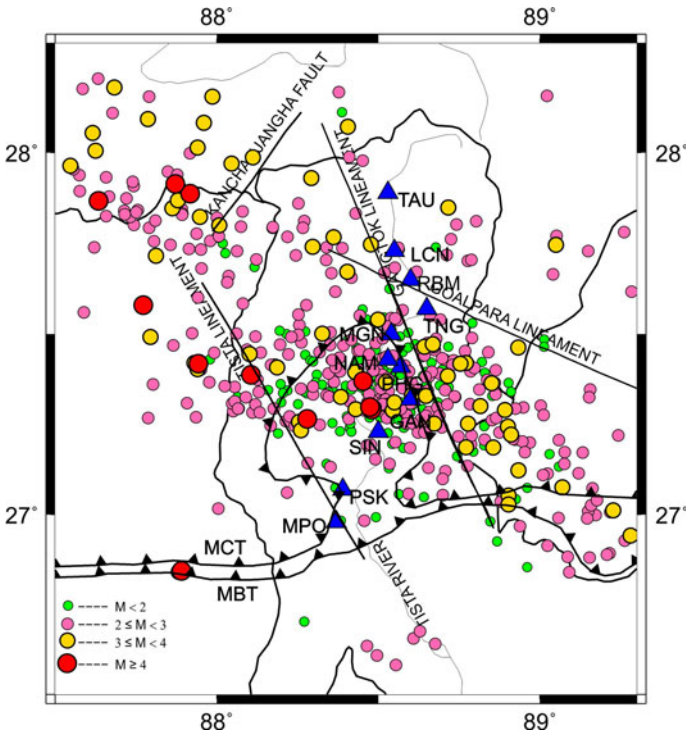
Fig. 1 Tectonic map of Sikkim region showing the stations (*triangles*) and epicenters of the all events selected for double-difference location. *MBT* main boundary thrust, *MCT* main central thrust (GSI 2000)

and after an earthquake. The stress drop is essentially constant as the earthquake moment increases, so that the ratio of slip to fault length remains the same. As a result, larger moment earthquakes have longer faults and hence lower corner frequencies. However, many observational studies reveal that the stress drop and seismic moment are independent of each other, and stress drops are log normally distributed (Allmann and Shearer 2009; Allen et al. 2004; Baltay et al. 2011). A global study using 17 years of earthquake data in the magnitude range from 5.2 to 8.3 revealed lack of dependency between seismic moments and stress drops, thus implying self-similarity of earthquakes on a global scale (Allmann and Shearer 2009). Albeit many studies, it is still unclear whether earthquakes obey self-similarity. While many studies propose that earthquakes are self-similar (e.g., Allmann and Shearer 2009; Prieto et al. 2004; Abercrombie 1995, etc.), contrary reports on breakdown of this process (e.g., Mayeda et al. 2007; Shi et al. 1998; Hough 1996) are also in vogue. A dependence of median stress drop on the earthquake source mechanism is also inferred by Allmann and Shearer (2009), with strike-slip earthquakes revealing higher stress drops and average corner frequencies compared with normal- and reverse-type earthquakes having equivalent scalar seismic moments. Further, the intraplate earthquakes have been found to possess higher stress drops when compared with interplate earthquakes (Allmann and Shearer 2009; Kato 2009). Recently, Yen and Ma (2011) observed an inverse relationship between stress drop and earthquake size for the Taiwan collision zone earthquakes having seismic moments less than 10^{20} Nm, contrary to other studies that reported an increase in stress drop with earthquake size (e.g., Fletcher 1980; Mandal et al. 1998; Shi et al. 1998; Drouet et al. 2008; Boore et al. 2010).

2 Estimation of hypocenters

The National Geophysical Research Institute has operated a network of seismic stations in the Sikkim region during the period October 2004–February 2010. The network comprised 11 broadband stations equipped with KS2000 M and STS2 seismometers connected to REFTEK 130 data acquisition systems. The data were recorded in continuous mode at the rate of 20 samples per second. As a sequel to our previous analysis of seismicity and tectonics of the region (Hazarika et al. 2010), we estimate the hypocentral parameters of earthquakes that occurred after December 2007, by analyzing the waveforms recorded by our network. Picking of the P- and S-wave arrival times required for the location of the local earthquakes has been done using the SEISAN software (Havskov and Ottemöller 2003). Based on our previous experience of locating earthquakes in the Sikkim region, a three-layer velocity model (Cotte et al. 1999) was utilized, since it yields the lowest root mean square (rms) location errors. Out of all the earthquakes recorded, a total of 344 shocks could be well located by the HYPOCENTER program. In order to further refine the hypocentral parameters, the double-difference (hypoDD) algorithm (Waldhauser 2001) has been utilized using the P and S arrival times of these 344 events together with those of the 356 events located by us earlier (Hazarika et al. 2010). The hypoDD algorithm has the advantage that it minimizes errors due to an unmodeled velocity structure without relying on the station corrections. If the hypocentral separation between two earthquakes is small compared to the event station distance and the scale length of the velocity heterogeneity, then the ray paths between the source region and a common station are similar along almost the entire ray path. In this case, the difference in travel times for two events observed at one station can be attributed to the spatial offset between the events with high accuracy. The parameterization was done adopting the following criteria: (1) the maximum distance between an event pair corresponding to a given station is 150 km; (2) the maximum hypocentral separation between event pairs is 6 km; (3) maximum number of neighbors per event is 8; and (4) the definition of a neighbor involves a minimum number of 6 links. On an average, a total of ten P and S differential times resulted in each event pair. Following these criteria, P and S arrival times of 602 out of the 700 events are used as inputs to hypoDD after assigning 100 % weight to P and 60 % weight for S-wave data. Figure 1 shows the epicenters of these selected events along with tectonic features and the seismic network in Sikkim Himalaya. Using the conjugate gradient method (LSQR), 360 events were relocated by hypoDD. Omission of a large number of events is primarily because poorly linked events have been discarded by hypoDD following the parameterization criteria mentioned above. A plot of the relocated events (Fig. 2) reveals two major clusters, one located between MBT and MCT and the other in the northwestern part of Sikkim where the Mw 6.9 September 18, 2011, occurred. Although there is no visible change in the epicenters of these relocated events when compared with the single-event locations, the average rms residual decreases from 0.1 to 0.01 s. The mean change in epicentral location is 4.2 km with the change in depth being 1 km.

3 Source parameters

In our earlier observations, it has been found that the tectonic character of the Sikkim Himalaya is different from the other segments of Himalaya (Hazarika et al. 2010), and this motivated us to determine the source parameters of earthquakes in Sikkim and compare them with those from the rest of the Himalaya. However, the Nyquist frequency of our data
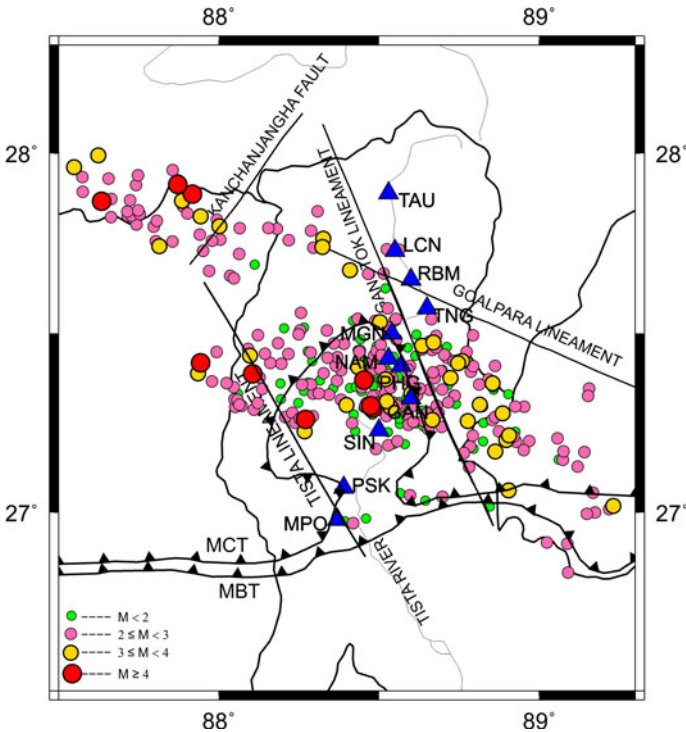
Fig. 2 Tectonic map of Sikkim region showing the stations (*triangles*) and epicenters of all the events relocated using hypoDD. *MBT* main boundary thrust, *MCT* main central thrust (GSI 2000)

set being 10 Hz, spectral analysis for corner frequencies beyond this becomes meaningless. Since the corner frequency for $M > 4$ earthquakes is well within 10 Hz, we restrict our analysis to only 9 events that fulfill this criterion. The procedure that we followed for source parameter estimation, using the SEISAN software (Havskov and Ottemöller 2003), is outlined in the following. The instrument corrected north–south and east–west components of the waveforms are rotated to radial and transverse components. A time window of 4–5 s (depending on clear observation of spectral decay) starting from the S-wave onset was selected on the transverse component to determine the Fourier spectra. The reason behind choosing only the transverse component is based on the observation that in the far field, the shear wave is predominantly present in the transverse component (Aki and Richards 2002). The displacement spectra are then approximated manually with the help of two straight lines, one corresponding to the flat level at low frequencies and the other to the omega-square decay for frequencies greater than the corner frequency (f_c), determined by the intersection of these two straight lines. Further, the observed spectra are compared with the theoretical ones obtained using the source model developed by Brune (1970). Most of the workers (Tucker and Brune 1977; Fletcher 1980; Archuleta et al. 1982; Hanks and Boore 1984; O'Neill 1984; Andrews 1986; Sharma and Wason 1994; Bansal 1998; Ottemoller and Havskov 2003) adopt the source model of Brune (1970) to compute source parameters like stress drop, seismic moment and source radius. The model describes the nature of seismic spectrum radiated from a seismic source by considering the physical process of the energy release. The displacement spectrum described in this model can be represented as

$$D(f,t) = \frac{M_0 * 0.6 * 2.0}{\left(1 + \left(\frac{f}{f_c}\right)^2\right) 4\pi\rho v^3} G(R) e^{-\pi f \kappa} e^{-\frac{\pi f t}{Q(f)}} \qquad (1)$$

where we used the factors 0.6 and 2.0 to account for the average radiation pattern and free surface effect, respectively, $\rho = 2.7 \times 10^3$ kg/m³, $v = 3.8 \times 10^3$ m/s, f_c is the corner frequency in Hz, M_0 is the seismic moment in Nm given by

$$M_0 = \frac{\Omega_0 4\pi\rho v_s^3}{0.6 * 2.0 * G(R)} \qquad (2)$$

where Ω_0 is the flat level of the spectrum.

$G(R)$ represents the geometrical spreading and can be expressed as (Herrmann and Kijko 1983)

$$G(R) = R^{-1} \text{for } R \le 100 \,\text{km and } G(R) = (100 \times R)^{-0.5} \text{for } R > 100 \,\text{km}.$$

The terms $e^{-\pi f \kappa} e^{-\frac{\pi f t}{Q(f)}}$ in Eq. (1) represent the attenuation correction. Of these, $e^{-\pi f \kappa}$ accounts for near-surface attenuation, and the second part $e^{-\frac{\pi f t}{Q(f)}}$ is correct for frequency-dependent attenuation along the path, t being the travel time in sec. In this study, we used $\kappa = 0.02$ s (Singh et al. 1982) and $Q(f) = 139 f^{1.2}$ obtained by analyzing the coda of S-waves from the Sikkim Himalaya (Manuscript under preparation) (Table 1).

The source radius r (km) and stress drop $\Delta\sigma$ (bar) are calculated as (Brune 1970; Eshelby 1957)

$$r = 0.37 v_s / f_c \qquad (3)$$

$$\Delta\sigma = \frac{7}{16} M_0 \frac{1}{r^3} * 10^{-14} \qquad (4)$$

The moment magnitude is calculated using the formula of Hanks and Kanamori (1979) as

$$M_w = \log M_0 / 1.5 - 6.06, \text{ where } M_0 \text{ is in Nm}. \qquad (5)$$

Figure 3 shows examples of the observed and theoretical spectra together with the corresponding seismograms. An average misfit value of ±0.032 suggests that the estimated parameters are well explained by the data. Trials using different window lengths reveal small changes in the source parameter estimates.

4 Results and discussion

4.1 Seismic moment (M_0)

Estimation of seismic moment is important to evaluate the size of an earthquake in terms of the moment magnitude (M_w). The seismic moments obtained in this study range between 7.95×10^{21} and 6.31×10^{23} dyne-cm. Smaller seismic moments obtained in the Sikkim Himalaya when compared with the rest of the Himalaya vindicates the low seismicity levels in the region with respect to the other parts of the Himalaya. Also, our data spanning 5 years have merely 9 events with magnitude greater than or equal to 4 with 5.3 being the maximum magnitude. Interestingly, it is observed

Table 1 Compilation of source parameters of earthquakes from the Himalayan region including those estimated in this study

| Region	Magnitude range (M_w)	Seismic moment (M_0) (dyne-cm)	Source radius (r) (km)	Corner frequency (f_c)(Hz)	Stress drop ($\Delta\sigma$) (bar)
Garhwal Himalaya (Sharma and Wason 1994)	1.4–4.2	7×10^{18}–6.23×10^{21}	0.347–0.545		0.04–38.49
Nepal Himalaya (Gupta and Singh 1980)	5.2–6.1	0.5×10^{25}–10.4×10^{25}	6.2–14.1	0.115–0.214	3.6–48.6
Himachal Himalaya (Ram et al. 2005)	5.4	2.1×10^{24}	2.8		36
Chamoli (Kumar et al. 2006)	6.4 (Main shock)	$(5.03 \pm 1.7) \times 10^{25}$	0.9–1.4		65
	4.7–4.9 (After shock)	1.4×10^{23}–2.9×10^{23}			23–153
Uttarkashi (Kumar et al. 2005)	6.7	1.7×10^{26}	11		53
Himalaya (Singh et al. 1978)	4.8–6.2	0.01×10^{25}–10.4×10^{25}	5.9–15.4	0.115–0.355	2.2–42.2
Burma (Singh et al. 1978)	4.4–5.9	0.2×10^{25}–13.3×10^{25}	6.2–22.4	0.1–0.355	0.3–67.8
Tibet (Singh et al. 1978)	4.8–5.5	2.1×10^{25}–26.7×10^{25}	8.9–17.3	0.129–0.288	5.5–91.7
Kunlun (Singh et al. 1978)	5.3–6.0	9.0×10^{25}–90.1×10^{25}	6.4–18.6	0.12–0.204	34.2–152.6
Garhwal Himalaya (Raj et al. 2009)	5.0 and 5.1	1.29×10^{23} and 6.95×10^{23}		1.6 and 2.0	1,370 and 385
Sikkim (Raj et al. 2009)	5.0–5.6	1.95×10^{21}–4.40×10^{22}		2.0–7.0	47–149
Sikkim (this study)	4.0–5.1	7.9×10^{21}–6.31×10^{23}	0.225–0.781	1.8–6.5	47.59–389.1
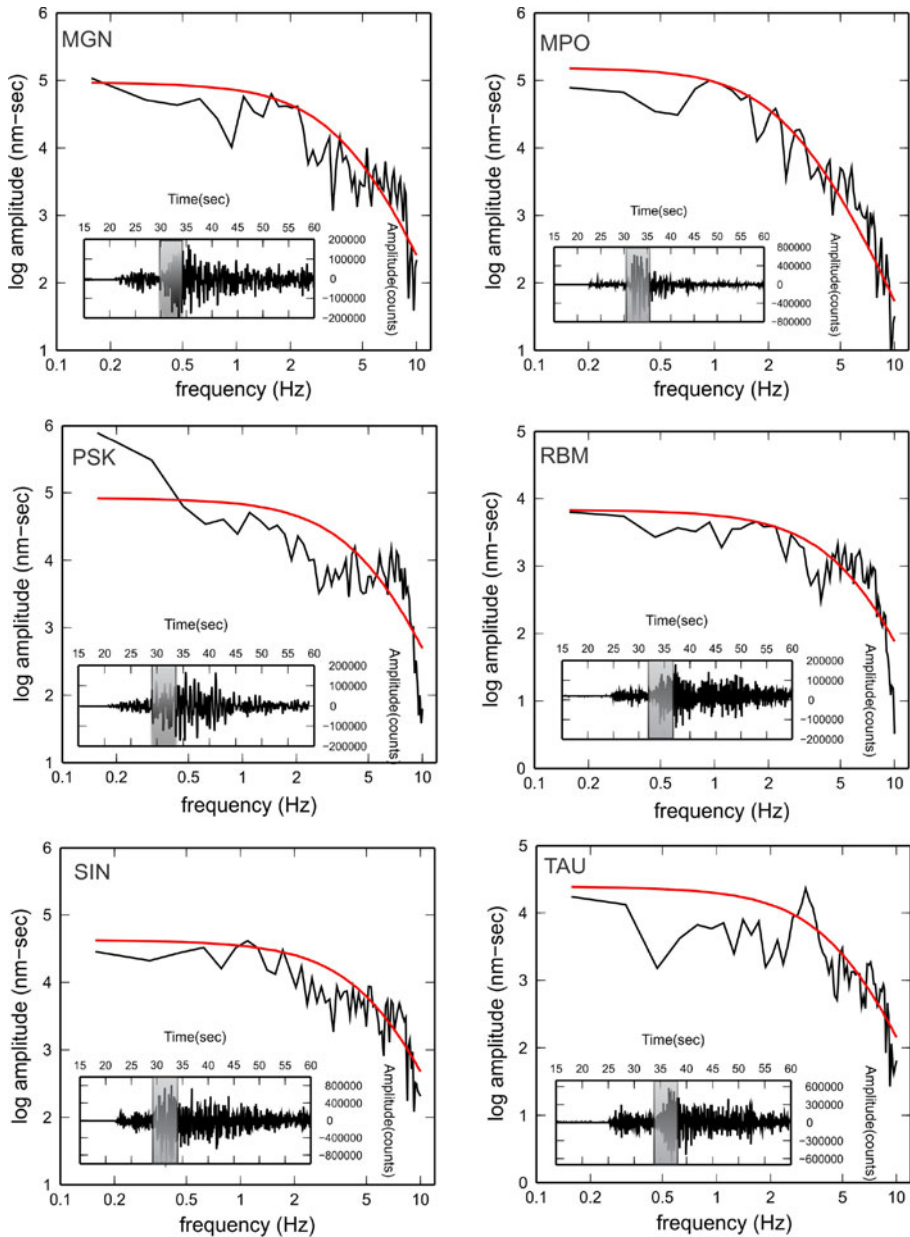
Fig. 3 Examples showing Fourier displacement spectra of shear waves due to an earthquake of M_w 4.3 on August 11, 2007 recorded at seismic stations MGM, MPO, PSK, SIN, RBM and TAU together with the respective transverse components of seismograms. *Gray shades* on the seismograms indicate the analysis windows. *Solid red lines* denote predicted spectral amplitudes (using Brune's model). Epicenter of the event and station locations are shown in Fig. 1

that most of the events having larger seismic moment occur between MBT and MCT, lending credence to our earlier observation that this is the most active portion of Sikkim Himalaya.

4.2 Corner frequency (f_c)

In a source parameter study, accurate determination of corner frequency is important, since other parameters like source radius, source duration and maximum slip velocity are directly derivable from it. The estimated corner frequencies in the study region vary from 1.8 to 6.25 Hz, the average value being 4.73 ± 1.16. The results reveal a linearity between corner frequencies and seismic moments ($M_0 \propto f_c^{-3.6}$; Fig. 4), similar to those found in other tectonic settings (e.g., Chouliaras and Stavrakakis 1997; Hiramatsu et al. 2002, etc.). Generally, corner frequency follows the scaling law $M_0 \propto f_c^{-3}$, indicating self-similarity of earthquakes, while stress drops are found to be independent over a wide moment range (Aki 1967). This is reiterated in a global study spanning a wide range of seismic moments (Allmann and Shearer 2009). However, there is a breakdown of self-similarity for earthquakes having smaller seismic moments (Abercrombie 1995). Hiramatsu et al. (2002) reported that micro earthquakes also follow the above-mentioned scaling law between seismic moment and corner frequency. However, they demonstrate that in the case of earthquakes with a low-frequency content, the relation $M_0 \propto f_c^{-4}$ becomes valid implying a breakdown of earthquake self-similarity, due to the absence of high-frequency component. Our results showing a deviation from the relation $M_0 \propto f_c^{-3}$ could be due to this effect.

4.3 Source radius (r)

The source radii estimated from the corner frequencies lie between 0.225 and 0.781 km. Logarithm of the source radii plotted against the logarithm of seismic moments (Fig. 5) broadly depicts a liner trend, in conformity with the previous studies that suggest a similar relationship for earthquakes within a magnitude range of 6–7 (Pearson 1982).

4.4 Stress drop ($\Delta\sigma$)

The stress drops obtained in this study vary from a low value of 47.6 bar to a high value of 389 bar. While most of the events have stress drops smaller than 100 bar, and only 2 events have stress drops more than 200 bar. Since most of the events have similar magnitudes, it

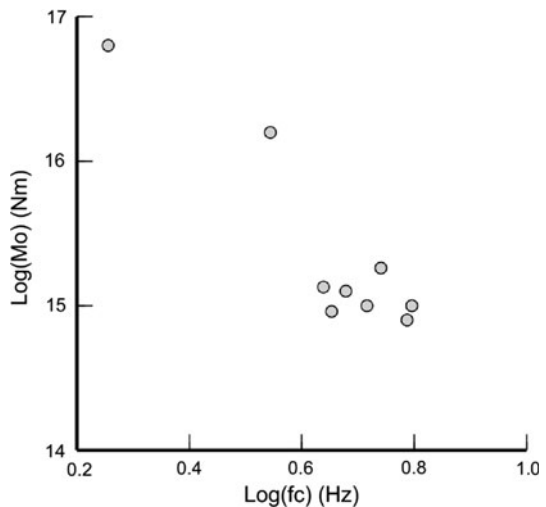**Fig. 4** Plot of logarithm of seismic moment versus corner frequency

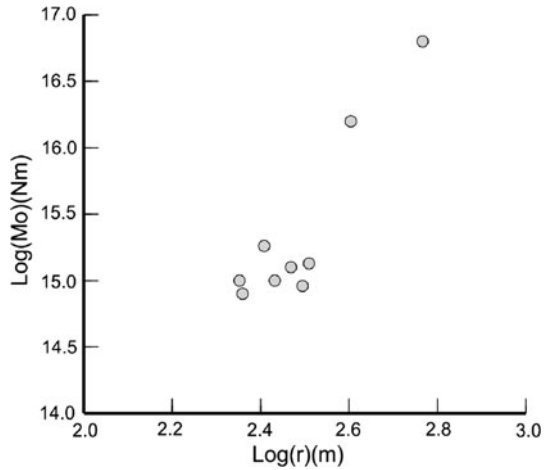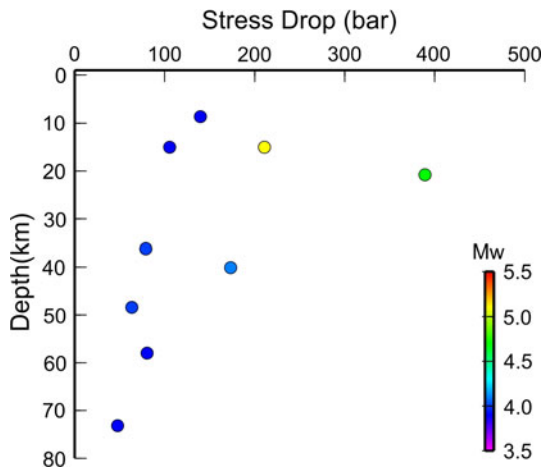**Fig. 5** Variation of logarithm of seismic moment with source radius

Fig. 6 Plot showing the variation of stress drop with hypocentral depth. The *circles* are *colored* based on the moment magnitude of the earthquake

is hard to establish a relation between magnitude and stress drop. Generally, it appears that the stress drops increase with magnitude and decrease with focal depth (Fig. 6). To understand the relation between stress drop and seismic moment in Sikkim Himalaya, the logarithm of seismic moment is plotted against stress drop (Fig. 7). It can be seen from the figure that the stress drop tends to increase with seismic moment, but does not follow any obvious trend, supporting the view that stress drop is independent of moment. In an earlier study, Raj et al. (2009) reported an average stress drop of 65 bar for Sikkim Himalaya using strong motion data from 12 earthquakes of $M_w \geq 5$. Stress drop of an earthquake may vary greatly according to its geological environment (Aki 1967). Generally, for most of the earthquakes, the stress drops lie in between 10 and 100 bars (Aki and Richards 2002). For the other parts of Himalaya like the Garhwal Himalaya, low stress drops with a maximum value of 38 bar (Sharma and Wason 1994) were reported. An extreme value of 385 bar (Raj et al. 2009) reported recently could be an outlier. Earlier, a wide range of stress drops (2.2–42 bar) have been reported for the Himalayan earthquakes (Singh et al. 1978). Within the Nepal Himalaya, the stress drops are found to vary between 3.6 and 48.6 bar for earthquakes in the magnitude range of 5.2–6.2 (Gupta and Singh 1980). It was

Fig. 7 Variation of stress drop with logarithm of seismic moment
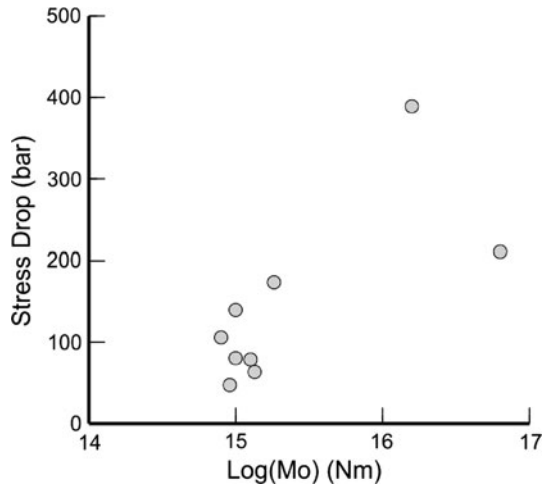
proposed that earthquakes from different tectonic regions have systematically different stress drops (Wyss and Brune 1971; Thatcher and Hanks 1973). A global study (Allmann and Shearer 2009) suggests that (1) intraplate earthquakes have higher stress drops than the interplate earthquakes; (2) among the latter ones, earthquakes from continental collision zones exhibit lower stress drops when compared with other tectonic regions; (3) stress drops are larger for the strike-slip earthquakes when compared with the other type of focal mechanisms. While the continental collision scenario can be invoked as a reason to explain the majority of events having low stress drop in the entire Himalayan region, those with a comparatively higher stress drop values within the Sikkim Himalaya (Fig. 8) could be due to the strike-slip mechanisms that are predominant in the region (Hazarika et al. 2010). Interestingly, the 20th May 2007 earthquake that shows the highest stress drop of 389 bar (in this study) is associated with a strike-slip source mechanism (Global CMT catalog). This value, although anomalous, seems to be well constrained, since variation of the window length does not significantly alter the estimate of stress drop.

4.5 Empirical relations

In order to establish a relation between scalar seismic moment (M_0) and local magnitude (Ml), the calculated M_0 are plotted against Ml (Fig. 9). Using a least square optimization approach at 95% confidence level, the relation between scalar seismic moment and magnitude is found to be $Log M_0 = (1.56 \pm 0.04)Ml + (8.55 \pm 0.12)$. Table 2 lists similar relations derived for other places in the world by various workers. These examples suggest that moment and magnitude relation varies locally and the empirical relation established for Sikkim Himalaya seems acceptable. The moment magnitude plotted as a function of local magnitude (Fig. 10) reveals a small difference between these two magnitudes. The empirical relationship obtained by a least square regression approach can be written as $M_w = (0.92 \pm 0.02)Ml + (0.14 \pm 0.06)$. Theoretically, Ml and M_w should be identical if the source process of all the earthquakes is similar and all the factors influencing the amplitude of observed waves, such as radiation pattern, path and site effects are properly accounted for. However, in practice, this is not the case, and the observed differences between M_w and Ml signify either the physical properties of the earthquake source
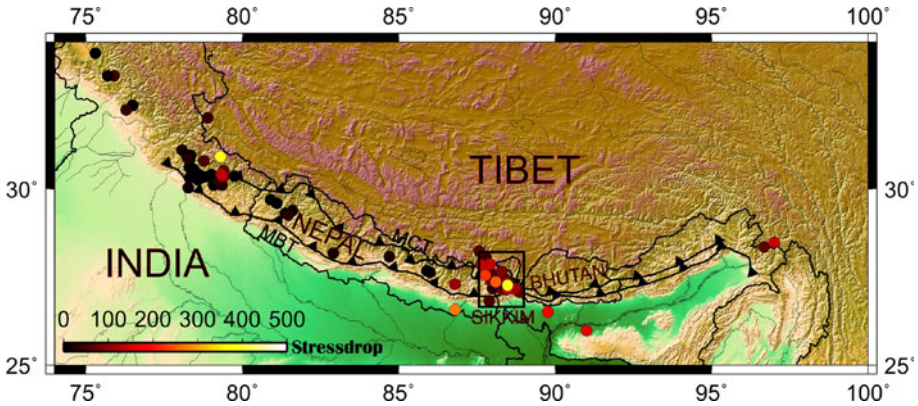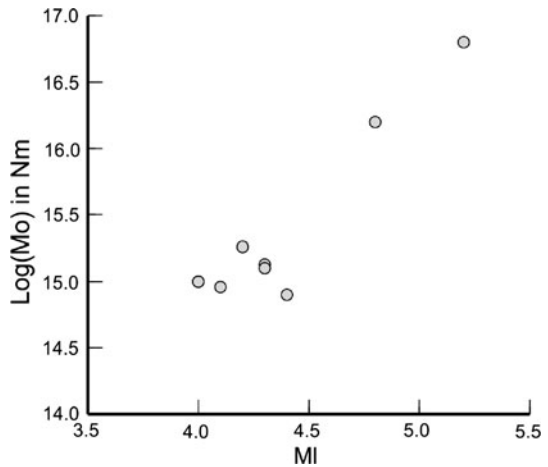
Fig. 8 Stress drop variations in different segments of Himalaya using data listed in Table 1. *Rectangle* demarcates the Sikkim region

Fig. 9 Richter local magnitude (Ml) versus logarithm of seismic moment (M_0)

or the inadequacies in our wave propagation model and means of measuring Ml (Deichmann 2006).

The relations that quantify the relation between (1) f_c and Ml and (2) f_c and M_w for the Sikkim region estimated by least square regression analysis of these parameters (Fig. 11) are as follows:

$$\text{Log}(f_c) = (-0.37 \pm 0.09)Ml + (2.26 \pm 0.21)$$
$$\text{Log}(f_c) = (-0.35 \pm 0.15)M_w + (2.11 \pm 0.4)$$

According to Brune (1970), the logarithm of corner frequency and moment magnitude are related as $\text{Log}(f_c) \, \alpha \, -0.5M_w$. A negative slope of 0.35 obtained by us for the Sikkim region is lower than the standard one. Such lower values have also been reported for other regions across the globe (Drouet et al. 2005, 2008; Chevrot and Cansi 1996). One possible reason for this could be because the scaling relation $M_0 \, \alpha \, f_c^{-3}$ law is not valid for the data set, and there is breakdown of earthquake self-similarity.

Table 2 Relation between local magnitude (Ml) and logarithm of seismic moment (M_0) for different tectonic settings across the globe

Region	Relation between Ml and $\text{Log}M_0$	Source
Garhwal Himalaya	$\text{Log}M_0 = (0.89 \pm 0.43)Ml + (18.18 \pm 0.21)$	Sharma and Wason (1994)
California	$\text{Log}M_0 = (1.36 \pm 0.22)Ml + (16.8 \pm 1.1)$ for $Ml \geq 4.3$ $\text{Log}M_0 = (1.1 \pm 0.14)Ml + (18 \pm 0.51)$ for $Ml \leq 4.1$	Fletcher et al. (1984)
San Andreas	$\text{Log}M_0 = 1.4Ml + 17.0$	Wyss and Brune (1968)
Southern California	$\text{Log}M_0 = 1.5Ml + 16.0$	Thatcher and Hanks (1973)
Koyna (India)	$\text{Log}M_0 = 1.018Ml + 17.597 \pm 0.361$	Gupta and Rambabu (1993)
Greece	$\text{Log}M_0 = (1.57 \pm 0.09)Ml + (16.22 \pm 0.39)$	Chouliaras and Stavrakakis (1997)
California	$\text{Log}M_0 = (1.16 \pm 0.06)Ml + (17.6 \pm 0.28)$	Johnson and McEvilly (1974)
Baltic shield	$\text{Log}M_0 = 1.01Ml + 16.93$ for $2 \leq Ml \leq 5.2$	Kim et al. (1989)
Sikkim Himalaya	$\text{Log}M_0 = (1.56 \pm 0.04)Ml + (8.55 \pm 0.12)$	This study

Fig. 10 Plot showing the relation between moment magnitude (M_w) and local magnitude (Ml)
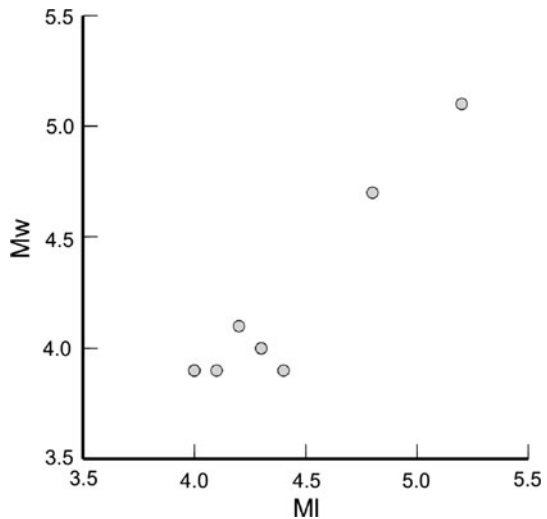
5 Conclusions

Application of the double-difference technique hypoDD and accurate relocation of 360 earthquakes in Sikkim using waveform data of 700 local earthquakes spanning 5 years reiterates the observation that seismicity in this segment of Himalaya is predominantly concentrated in the region between MBT and MCT. Interestingly, a cluster of events is observed to the northwest of Sikkim, which is host to the recent Mw6.9 devastating earthquake of September 11, 2011. Further, estimates of source parameters of 9 earthquakes having $M \geq 4$ reveal that seismic moments are related to the corner frequencies as $M_0 \propto f_c^{-3.6}$, and they do not correlate with the stress drop. Higher stress drops for earthquakes in this segment of Himalaya could be due to the strike-slip nature of faulting that contrasts with a predominance of thrust faulting in the rest of the Himalaya. Least square regression of the scalar seismic moment (M_0) and local magnitude (Ml) results in a relation
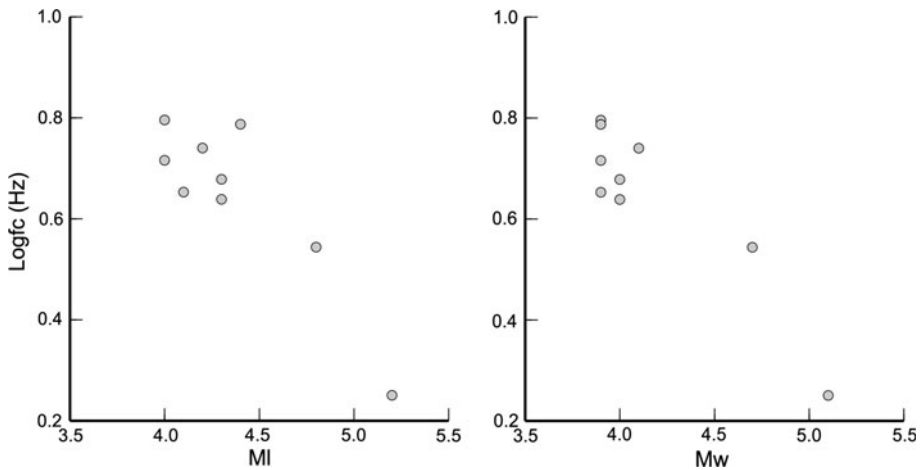
Fig. 11 Logarithm of corner frequency plotted against local and moment magnitudes

$LogM_0 = (1.56 \pm 0.05)Ml + (8.55 \pm 0.12)$ while that between moment magnitude (M_w) and local magnitude as $M_w = (0.92 \pm 0.04)Ml + (0.14 \pm 0.06)$.

References

Abercrombie RE (1995) Earthquake source scaling relationship from −1 to 5 M_L using seismograms recorded at 2.5-km depth. J Geophys Res 100:24015–24036

Aki K (1967) Scaling law of seismic spectrum. Bull Seismol Soc Am 72:1217–1231

Aki K, Richards PG (2002) Quantitative seismology, 2nd edn. University Science Books, Sausalito, CA

Allen I, Trevor Gibson G, Brown A, Cull JP (2004) Depth variation of seismic source scaling relations: implications for earthquake hazard in southeastern Australia. Tectonophysics 390:5–24

Allmann BP, Shearer PM (2009) Global variation of stress drop for moderate to large earthquakes. J Geophys Res 114:B-131. doi:10.1029/2008JB005821

Andrews DJ (1986) Objective determination of source parameters and similarity of earthquakes of different size. In: Das et al. (Eds) Earthquake source mechanics. Ewing Series, 6, AGU, Washington DC www1986, pp 259–267

Archuleta RJ, Cranswick E, Mueller C, Spudich P (1982) Source parameters of the 1980 Mammoth Lakes. California, earthquake sequence. J Geophys Res 87:4595–4607

Baltay A, Ide S, Prieto G, Beroza G (2011) Variability in earthquake stress drop and apparent stress. Geophys Res Lett 38:L06303. doi:10.1029/2011GL046698

Bansal BK (1998) Determination of source parameters for small earthquake in the Koyna region, 11th symposium on earthquake engineering. Roorkee 1:57–66

Boatwright J (1980) A spectral theory for seismic sources: simple estimates of source dimension, dynamic stress drop and radiator energy. Bull Seism Soc Am 70:1–27

Boore DM, Campbell WC, Atkinson GM (2010) Determination of stress parameters for eight well-recorded earthquakes in Eastern North America. Bull Seism Soc Am 100:1632–1645. doi:10.1785/0120090328

Brune JN (1970) Tectonic stress and seismic shear waves from earthquakes. J Geophys Res 75:4997–5009

Brune JN (1971) Correction. J Geophys Res 76:5002

Chevrot S, Cansi Y (1996) Source spectra and site-response estimates using the coda of Lg waves in western Europe. Geophys Res Lett 23:1605–1608

Chouliaras G, Stavrakakis GN (1997) Seismic source parameters from a new dial-up seismological network in Greece. Pure Appl Geophys 150:91–111

Cotte N, Pedersen H, Campillo M, Mars J, Ni J, Kind R, Sandvol E, Zhao W (1999) Determination of the crustal structure in Southern Tibet by dispersion and amplitude analysis of Rayleigh waves. Geophys J Int 138:809–819

Deichmann N (2006) Local magnitude. A moment revisited. Bull Seism Soc Am 96:1267–1277. doi: 10.1785/0120050115

Drouet S, Souriau A, Cotton F (2005) Attenuation, seismic moment, and site effects for weak-motion events: application to the Pyrenees. Bull Seismol Soc Am 95(5):1731–1748

Drouet S, Chevrot S, Cotton F, Souriau A (2008) Simultaneous Inversion of Source Spectra, Attenuation Parameters and Site Responses: Application to the data of the French Accelerometric Network. Bull Seism Soc Am 98:198–219. doi:10.1785/0120060215

Drukpa D, Velasco AA, Doser DI (2006) Seismicity in the Kingdom of Bhutan (1937–2003): evidence for crustal transcurrent deformation. J Geophys Res B Solid Earth Planets 111:B06301

Eshelby J (1957) The determination of the elastic field of an ellipsoidal inclusion and related problems. Proc R Soc Lond A 241:376–396

Fletcher JB (1980) A comparison between high-dynamic range digital recordings of Oroville, California aftershocks and their source parameters. Bull Seism Soc Am 70:735–755

Fletcher JB, Boatwright J, Harr L, Hanks T, McGarr A (1984) Source parameters for aftershocks of the Oroville, California earthquake. Bull Seism Soc Am 74:1101–1123

GSI (2000) Seismotectonic Atlas of India and its environs

Gupta DI, Rambabu V (1993) Source parameters of some significant earthquakes near Koyna Dam, India. Pageop 140:403–413

Gupta HK, Singh DD (1980) Spectral analysis of body waves for earthquakes in Nepal Himalaya and vicinity: their focal parameters and tectonic implications. Tectonophysics 62:53–66

Hanks TC, Boore DM (1984) Moment-Magnitude relations in theory and practice. J Geophys Res 89:6229–6235

Hanks TC, Kanamori H (1979) A moment magnitude scale. J Geophys Res 84:2348–2350

Havskov J, Ottemöller L (2003) SEISAN: the earthquake analysis software, version 8.0, Institute of Solid Earth Physics, University of Bergen, Bergen, Norway

Hazarika P, Kumar MR, Srijayanthi G, Raju PS, Rao NP, Srinagesh D (2010) Transverse Tectonics in Sikkim Himalaya: evidences from seismicity and focal mechanism data. Bull Seism Soc Am 100:1816–1822. doi:10.1785/0120090339

Herrmann RB, Kijko A (1983) Modelling some empirical vertical component Lg relations. Bull Seismol Soc Am 75:157–171

Hiramatsu Y, Yamanaka H, Tadokoro K, Nishigami K, Ohmi S (2002) Scaling law between corner frequency and seismic moment of microearthquakes: is the breakdown of cube law a nature of earthquake? Geophys Res Lett 29:1211. doi:10.1029/2001GL013894

Hough SE (1996) Observational constraints on earthquake source scaling: understanding the limits in resolution. Tectonophysics 261:83–95

Johnson LR, McEvilly TV (1974) Near field observations and source parameters of Central California earthquakes. Bull Seismol Soc Am 64:1855–1886

Kato N (2009) A possible explanation for difference in stress drop between intraplate and interplate earthquakes. Geophys Res Lett 36:L23311. doi:10.1029/2009GL040985

Kayal JR, Baruah S, Baruah S, Gautam JL, Arefiev SS, Tatevossian R (2011) The September 2011 Sikkim deeper centroid Mw 6.9 earthquake: role of transverse faults in eastern Himalaya, DCS-DST News

Kim WY, Wahlstrom R, Uski M (1989) Regional spectral scaling relations of source parameters for earthquakes in the Baltic Shield. Tectonophysics 166:151–161

Kumar D, Ram VS, Khattri KN (2006) A study of source parameters, site amplification functions and average effective shear wave quality factor qseff from analysis of accelerograms of the 1999 Chamoli earthquake, Himalaya. Pure Appl Geophys 163:1369–1398

Kumar D, Sarkar I, Sriram V, Khattri KN (2005) Estimation of the source parameters of the Himalaya earthquake of October 19, 1991, average effective shear wave attenuation parameter and local site effects from accelerograms. Tectonophysics 407:1–24

Mandal PK, Rastogi BK, Sarma CSP (1998) Source parameters of Koyna earthquakes, India. Bull Seism Soc Am 88:833–842

Mayeda K, Malagnini L, Walter WR (2007) A new spectral ratio method using narrow band coda envelopes: evidence for non-self-similarity in the Hector Mine sequence. Geophys Res Lett 34:L11303. doi:10.1029/2007GL030041

O'Neill ME (1984) Source dimension and stress drops of small earthquakes near Parkfield, California. Bull Seism Soc Am 71:27–40

Ottemoller L, Havskov J (2003) Moment magnitude determination for local and regional earthquakes based on source spectra. Bull Seism Soc Am 93:203–214

Pearson C (1982) Parameters and a magnitude moment relationship for small earthquakes observed during hydraulic fracturing experiments in crystalline rocks. Geophys Res Lett 9:404–407

Prieto GA, Shearer PM, Vernon FL, Kilb D (2004) Earthquake source scaling and self-similarity estimation from stacking P and S spectra. J Geophys Res 109:B08310. doi:10.1029/2004JB003084

Raj A, Nath SK, Bansal BK, Thingbaijam KKS, Kumar A, Thiruvengadam N, Yadav A, Arrawatia ML (2009) Rapid estimation of source parameters using finite fault modeling-Case studies from the Sikkim and Garhwal Himalayas. Seism Res Lett 80(1):89–96

Rajendran K, Rajendran CP, Thulasiraman N, Andrews R, Sherpa N (2011) The 18 September, North Sikkim earthquake: a preliminary report. Curr Sci 101:1475–1479

Ram VS, Kumar D, Khattri KN (2005) The 1986 Dharamsala earthquake of Himachal Himalaya – estimates of source parameters, average intrinsic attenuation and site amplification functions. J Seismol 9:473–485

Sharma ML, Wason HR (1994) Occurrence of low stress drop earthquakes in the Garhwal Himalaya region. Phys Earth Planet Inter 85:265–722

Shi J, Kim WY, Richards PG (1998) The corner frequencies and stress drops of intraplate earthquakes in the Northeastern United States. Bull Seism Soc Am 88:531–542

Singh DD, Rastogi BK, Gupta HK (1978) Spectral analysis of body waves for earthquakes and their source parameters in the Himalaya and nearby regions. Phys Earth Planet Inter 18:143–152

Singh SK, Apsel RJ, Fried J, Brune JN (1982) Spectral attenuation of SH-waves along the Imperial fault. Bull Seism Soc Am 72:2003–2016

Thatcher W, Hanks TC (1973) Source parameters of southern California earthquakes. J Geophys Res 78:8547–8576

Tucker BE, Brune JN (1977) Source mechanism and m_b–M_s analysis of aftershocks of the San Fernando earthquake. Geophys J 74:6617–6672

Waldhauser F (2001) HypoDD—a program to compute double-difference hypocenter locations. US Geol Survey Open File Report 113:1–25

Wyss M, Brune JN (1968) Seismic moment, stress and source dimensions for earthquakes in the California-Nevada region. J Geophys Res 73:4681–4694

Wyss M, Brune JN (1971) Regional variation of source properties in southern California estimated from the ratio of short to long period amplitudes. Bull Seismol Soc Am 61:1153–1168

Yen YT, Ma KF (2011) Source-scaling relationship for M 4.6-8.9 earthquakes, specifically for earthquakes in the collision zone of Taiwan. Bull Seismol Soc Am 101:464–481. doi:10.1785/0120100046